# Microelectrode Measurements of Local Mass Transport Rates in Heterogeneous Biofilms

**Kjetil Rasmussen,* Zbigniew Lewandowski**

*Center for Biofilm Engineering, 409 Cobleigh Hall, P.O. Box 173980, Montana State University-Bozeman, Bozeman, Montana 59717-3980; telephone: 406-994-5915; fax: 406-994-6098; e-mail: ZL@erc.montana.edu*

*Received 14 February 1997; accepted 2 December 1997*

**Abstract:** Microelectrodes were used to measure oxygen profiles and local mass transfer coefficient profiles in biofilm clusters and interstitial voids. Both profiles were measured at the same location in the biofilm. From the oxygen profile, the effective diffusive boundary layer thickness (DBL) was determined. The local mass transfer coefficient profiles provided information about the nature of mass transport near and within the biofilm. All profiles were measured at three different average flow velocities, 0.62, 1.53, and 2.60 cm $sec^{-1}$, to determine the influence of flow velocity on mass transport. Convective mass transport was active near the biofilm/liquid interface and in the upper layers of the biofilm, independent of biofilm thickness and flow velocity. The DBL varied strongly between locations for the same flow velocities. Oxygen and local mass transfer coefficient profiles collected through a 70 μm thick cluster revealed that a cluster of that thickness did not present any significant mass transport resistance. In a 350 μm thick biofilm cluster, however, the local mass transfer coefficient decreased gradually to very low values near the substratum. This was hypothetically attributed to the decreasing effective diffusivity in deeper layers of biofilms. Interstitial voids between clusters did not seem to influence the local mass transfer coefficients significantly for flow velocities of 1.53 and 2.60 cm $sec^{-1}$. At a flow velocity of 0.62 cm $sec^{-1}$, interstitial voids visibly decreased the local mass transfer coefficient near the bottom.  *Biotechnol Bioeng* **59**: 302–309, 1998.
**Keywords:** biofilms; microelectrodes; local mass transfer coefficient; effective diffusivity

## INTRODUCTION

Recent studies of biofilm architecture strongly influence our concepts of mass transport mechanisms within biofilms. Images of living biofilms, obtained using scanning confocal laser microscopy (SCLM), show that biofilms form cellular clusters separated by interstitial voids filled with either water or biopolymers (Keevil and Walker, 1992; Korber et al., 1994; Lawrence et al., 1991; Wolfaardt et al., 1994). It is well known that the nonuniform distribution of biomass in biofilms may influence the mass transport mechanism. Reports of such influences were published even before we fully realized the importance of biofilm architecture. The study of the nature of oxygen distribution within structurally heterogeneous biofilms clearly demonstrated the importance of biofilm architecture to oxygen transport (De Beer et al., 1994a). Siegrist and Gujer (1985) observed an increased average diffusion coefficient with increasing biofilm thickness and hypothesized that this occurs as a result of irregularities of thick biofilms penetrating the boundary layer and causing eddy diffusion. A similar mechanism may explain the observations reported by Larsen and Harremoës (1994) and Horn and Hempel (1995) who found the oxygen diffusion coefficient within a biofilm to be higher than in pure water. The concept of structurally heterogeneous biofilms constitutes an intellectual platform to accommodate these observations, which would otherwise be difficult to interpret. At the recent meeting of the International Association on Water Quality (IAWQ) Specialist Group on Biofilm Systems in Leeuwenhorst, the Netherlands, biofilm heterogeneity was informally defined as ''spatial differences in any parameter we think is important'' (Bishop and Rittmann, 1995).

Despite the awareness of biofilm heterogeneity, there is no clear consensus on what causes it, or of how the heterogeneity influences biofilm processes. Van Loosdrecht et al. (1995) discussed the influence of substrate loading rate, shear, and growth rate on the biofilm structure. Some qualitative opinions of how the process parameters influence biofilm structure have been established among biofilm researchers. For example, a high shear rate tends to increase biofilm density and mechanical stability. Higher substrate loadings and the presence of fast growing microorganisms both result in thicker, ragged biofilms. Some researchers initiated quantification of parameters influencing structural heterogeneity. Zhang and Bishop (1994a,b) determined the densities, porosities, specific surface areas, and mean pore radii of biofilms. In addition, they determined the distribution of the tortuosity factor and the ratio of the effective diffusivity in a biofilm to diffusivity in the bulk solution. Fu

* *Present address:* Department of Biotechnology, The Norwegian University of Science and Technology, N-7034, Trondheim, Norway.
*Correspondence to:* Zbigniew Lewandowski
Contract grant sponsors: National Science Foundation; Montana State University
Contract grant numbers: Cooperative Agreement EEC-8907039

 CCC 0006-3592/98/030302-08

et al. (1994) estimated the effective diffusivity in different layers of a biofilm using a dissolved oxygen microelectrode. Hermanowicz et al. (1995) used SCLM images to estimate the fractal dimension and biofilm morphology.

Biofilm reactivity is controlled by the rate of substrate consumption and by the rate of mass transport. Mass transport in biofilms is traditionally described using the film theory which assumes the presence of a fictitious film of fluid in laminar flow next to the boundary. The fictitious film provides the same amount of mass transfer resistance as actually exists in the flowing fluid. Hence, all mass transfer resistance exists in this fictitious film in which mass transport only occurs as molecular diffusion (Welty et al., 1976). Revsbech and Jørgensen (1986) refer to this film as the effective diffusive boundary layer (*DBL*). Lewandowski (1994) developed a method for calculating the thickness of the *DBL* from substrate concentration profiles. According to the film theory, the flux of substrate to a biofilm can be described using finite differences in Fick's diffusion equation:

$$J = D\,\frac{\Delta C}{DBL} \tag{1}$$

where $J$ is flux (mol $m^{-2}$ $sec^{-1}$), $D$ is the diffusion coefficient of the substrate in stagnant water ($m^2$ $sec^{-1}$), $\Delta C$ is the difference in the solute concentration (mol $m^{-3}$) between the bulk liquid and at the reacting surface, and *DBL* is the thickness of the effective diffusive boundary layer (m). From this definition, the mass transfer coefficient is the ratio of the diffusion coefficient to the thickness of the *DBL*, $k = D/DBL$. The value of the mass transfer coefficient depends on many factors, with hydrodynamics being the most significant, because flow velocity influences the thickness of the *DBL*. The higher the flow velocity, the thinner the *DBL*.

Experiments have demonstrated the true nature of hydrodynamics near biofilms. Lewandowski et al. (1993) used Nuclear Magnetic Resonance Imaging (NMRI) to show that water was moving in the space occupied by the biofilm. This study was followed by quantification of the intrabiofilm flow using a combination of particle tracking and SCLM. De Beer et al. (1994b) and Stoodley et al. (1994) determined the flow velocity profiles in voids and channels. The flow in biofilms occurs in two flow fields—one inside and one outside the biofilm (Lewandowski et al., 1995). The external and internal flow fields influence each other in a complex way. These studies indicate that direct application of the film theory may be confounding and demonstrate that the mass transport in biofilms is affected by convection to a much larger extent than previously suspected. Because of complex hydrodynamics, the intensity of convective mass transport in biofilms is difficult to quantify. To address this problem, Yang and Lewandowski (1995) developed a microtechnique to evaluate the local mass transfer coefficient in biofilms by measuring the limiting current drawn from a mobile microelectrode. The limiting current technique, based on the reduction of dissolved electroactive species at a cathodically polarized electrode, is often used to determine mass transfer rates to surfaces (Dawson and Trass, 1972; Hanratty, 1991; Juhasz and Deen, 1993). The concept of local mass transport coefficient introduced by Yang and Lewandowski (1995) results directly from the limiting current technique with the exception of using a mobile electrode, instead of a stationary one, to measure the limiting current. The flux of electroactive species to a polarized electrode is:

$$J = k\,(C_O - C_S) \tag{2}$$

where $C_O$ is the concentration of the reacting species in the bulk, and $C_S$ is the concentration of the reacting species at the surface of the microelectrode. The flux of electroactive species may be calculated from the polarization current:

$$J = \frac{I}{nAF} \tag{3}$$

where $I$ is the polarization current, $A$ is surface area of the electrode, and $n$ is number of moles of electrons transferred in the electrode reaction. Equations (2) and (3), when solved for the mass transfer coefficient, yield:

$$k = \frac{I}{nAF\,(C_O - C_S)} \tag{4}$$

During the local mass transfer coefficient measurements, the polarization potential of the electrode is fixed at a potential which causes the concentration of electroactive species at the electrode surface ($C_S$) to be zero—a state referred to as the limiting current condition. This situation is easily recognized, because a further increase in the polarization potential does not increase the current (within limits, of course). Having $C_S = 0$ simplifies equation (4) and allows for the calculation of the mass transport coefficient ($k$) from the measured parameters. The calculated mass transfer coefficient is called the local mass transport coefficient—the mass transport coefficient which reflects the resistance of mass transport to the tip of the microelectrode. The local mass transport coefficient should not be confused with the overall mass transport coefficient which controls the mass transport rate to the biofilm surface through the *DBL* [see eq. (1)]. The latter (overall) mass transport coefficient can be evaluated from the substrate concentration profiles measured by substrate specific microelectrodes. The local mass transfer coefficient reflects the mass transfer resistance in the immediate vicinity of the electrode tip, and thus is sensitive to the local hydrodynamics, local effective diffusivity (biofilm density), and biofilm architecture. Yang and Lewandowski (1995) reported that the local mass transfer coefficient varied both horizontally and vertically within biofilms.

To study the nature of mass transport near and within biofilms, we combined the measurements of the local mass transfer coefficients with the measurements of local dissolved oxygen concentrations. A bacterial biofilm com-

posed of aerobic microorganisms was grown in an open channel flow reactor. Profiles of dissolved oxygen were measured at different flow velocities, through the cell clusters, and through the interstitial voids. Subsequently, the growth medium was replaced with a ferricyanide solution, the local mass transfer coefficient profiles were measured at the same locations. Superimposing the two profiles indicates the effects of biofilm architecture and hydrodynamics on the rate of oxygen transport.

## MATERIALS AND METHODS

The experimental set-up was similar to that described by Yang and Lewandowski (1995). The biofilm was grown in an open channel reactor 40 mm wide by 500 mm long made of polycarbonate. A concentrated nutrient solution and filtered tap water (PAC-filter, Model CBC-10, Cole-Parmer Instr. Co., Chicago, IL) was aerated in a mixing chamber before it was recycled through the reactor by a peristaltic pump (Cole-Parmer Instr. Co., Chicago, IL). The influent nutrient solution from the mixing chamber consisted of $KH_2PO_4$ (0.69 m*M*), $K_2HPO_4$ (1.5 m*M*), $(NH_4)_2SO_4$ (0.079 m*M*), $MgSO_4$*$7H_2O$ (0.013 m*M*), and yeast extract (0.031 g $L^{-1}$). The total reactor volume was 420 mL, and the hydraulic retention time was only 4 min and 30 sec to avoid suspended growth. One-mL portions of stock cultures of *Pseudomonas aeruginosa* ($7.7 \times 10^9$ CFU/mL), *Pseudomonas fluorescens* ($4.8 \times 10^{10}$ CFU/mL), and *Klebsiella pneumoniae* ($7.2 \times 10^{10}$ CFU/mL) were used to inoculate the reactor. After inoculation, the reactor was operated in a batch mode for 24 h, followed by continuous flow mode for 5 d at room temperature. During the period of continuous flow, the reactor was tilted to obtain a shallow water depth, and hence, a high volumetric flow velocity set to 17 cm $sec^{-1}$. The high flow velocity during the growth phase was used to obtain biofilms of high density which were strongly attached to the bottom. This was necessary to avoid detachment or change of structure during the experiments in which a range of different microelectrodes, flow velocities, and solutions were used. After the biofilm was established, the reactor was positioned horizontally and the measurements were conducted at flow velocities of 0.62, 1.53, and 2.60 cm $sec^{-1}$.

Oxygen profiles were measured by a combined dissolved oxygen and reference microelectrode. The electrode was constructed as described by Revsbech (1989b). The oxygen sensor consisted of a 100 μm 99.99% pure platinum wire (California Wire Company, Grover Beach, CA), etched on one end to a diameter of 5 μm and covered by Schott 8533 glass (Schott Glaswerke, F.R.G.). The tip was exposed with a heating loop, and then goldplated. A 0.5 mm diameter, 99.99% pure silver wire, coated with an AgCl layer, was used as the silver/silver chloride reference electrode. The guard cathode was made from a 100 μm diameter, 99.99% pure silver wire (California Fine Wire Company, Grover Beach, CA). It was then fixed in a thin glass capillary. Approximately 1.5 cm of the wire was sticking out of the capillary on both ends. The oxygen sensor, the reference electrode, and the guard cathode were mounted inside a 5¾ inch long Pasteur Pipet (Fisher Scientific, Pittsburgh, PA) tapered to 10 μm at one end. A 10 μm thick uncured silicone membrane was applied on the tapered tip. The shaft was filled with electrolyte containing $K_2CO_3$ (0.3*M*), $KHCO_3$ (0.2*M*), and KCl (1.0*M*), then sealed with epoxy.

Microelectrodes to measure profiles of the local mass transfer coefficient were constructed following the procedure of Yang and Lewandowski (1995). Microelectrodes were made of 100 μm (pure TC grade) platinum wire (California Wire Company, Grover Beach, CA), with the tips etched electrochemically in 2*M* KCN solution to a diameter of less than 1 μm. The glass capillary was positioned in a Micro Electrode Puller (Stoelting Co., Wooddale, IL), while the tip of the wire was positioned 1 to 1.5 cm above the heating coil. Heat was gradually increased until the glass around the platinum wire melted and adhered to the wire while the entire capillary dropped down and cooled in the air. The tip of the wire was then exposed by grinding on a rotating diamond wheel (Model EG-4, Narishige Co, Tokyo, Japan). Tip diameter was measured microscopically to calculate the surface area of the electrode. The counter-reference electrode was a commercial calomel electrode (Model 13-620-51, Fisher Scientific, Pittsburgh, PA).

A micromanipulator (Model M3301L, World Precision Instruments, New Haven, CT) was used to move the microelectrodes. It was equipped with a stepper motor (Model 18503, Oriel, Stratford, CT) and manipulated by a computer controller (Model 20010, Oriel, Stratford, CT). The electrodes were moved from the bulk liquid down through the biofilm in 10 μm increments. The measured signal was directed to a computer containing a data acquisition system. Dissolved oxygen profiles were measured first. After the measurement, the nutrient solution was replaced by a solution of the electroactive species. Local mass transfer coefficient profiles were measured at the same locations as the dissolved oxygen profiles. The reactor was fixed to an X-Y micropositioner stage (Model CTC-462-2S, MicroKinetics, Laguna Hills, CA). The stage was computer controlled through a controller (Model CTC-283-3, MicroKinetics, Laguna Hills, CA). A computer equipped with custom-made software was used to control the stage movement. Before each set of measurements, a reference point was selected on the substratum using an inverted microscope (Model CK-2, Olympus, Japan), and the DO-probe was positioned directly above this point with a precision of 10 μm. The reactor departure from the reference point in the X and Y directions was then recorded. At each location, DO-profiles were collected for different volumetric flow velocities. The inverted microscope was also used to locate the tip of the microelectrode and to observe when the electrode reached the substratum. Before the local mass transfer coefficient measurements were taken, the reactor was drained, and a solution containing 25 m*M* potassium ferricyanide and 0.5*M* potassium chloride as supporting electrolyte was added. It was recycled through the reactor for 30 min to obtain a constant

ferricyanide concentration throughout the biofilm. The reference point was again found under the microscope, and the local mass transfer coefficient electrode was positioned above it with a precision of 10 μm. The reactor was then moved by the X-Y stage to the same locations at which the DO profiles were collected, and local mass transfer coefficient profiles were measured for the same flow velocities. The data acquisition system (Model CIO-DAS08PGL, Computer Boards, Inc., Mansfield, MA) collected current data from the Picoammeter/DC Voltage Source (Hewlett Packard 4140B). On the computer monitor, the vertical profiles of oxygen or local mass transfer coefficient were displayed in real time. At each step, 22 current readings were collected at a frequency of 1 KHz. The highest and lowest were rejected and a standard deviation was calculated for the remaining 20 readings. If the deviation was higher than 5%, the measurement at that location was repeated.

During the local mass transfer coefficient measurements, a potential of −0.8 volts was applied between the microelectrode and the reference electrode. As a result, ferricyanide diffused to the tip of the electrode and was reduced to ferrocyanide:

$$Fe(CN)_6^{3-} + e^- \rightarrow Fe(CN)_6^{4-} \quad (5)$$

The current drawn by the electrode was proportional to the local mass transfer coefficient:

$$k = I/nAFC_0 \quad (6)$$

where $k$ is the local mass transfer coefficient, $I$ is the limiting current, $n$ is the number of electrons transferred in the reaction [one from eq. (5)], $A$ is the sensing area of the microelectrode, $F$ is Faraday's constant, and $C_0$ is the ferricyanide concentration in the bulk solution.

Lewandowski et al. (1993, 1994) demonstrated that the shape of oxygen profiles in biofilms may be described by the following equation:

$$\frac{C - C_s}{C_b - C_s} = 1 - \exp\left[-B(X - X_s)\right] \quad (7)$$

where $C$ is the local substrate concentration, $C_s$ is the substrate concentration at the biofilm surface, $C_b$ is the bulk substrate concentration, $B$ is an experimental coefficient, $X$ is the distance from the substratum to the biofilm surface (biofilm thickness), and $(X - X_s)$ is the distance measured from the biofilm surface toward the bulk liquid phase. This equation can be linearized to conveniently calculate the coefficient $B$ from experimental data:

$$\mathrm{Ln}\left(1 - \frac{C - C_s}{C_b - C_s}\right) = -B\,(X - X_s) \quad (8)$$

We used $1/B$ as a measure of the *DBL* thickness (Lewandowski et al., 1993).

## RESULTS AND DISCUSSION

The biofilm was grown at a flow velocity of 17 cm $sec^{-1}$ (Reynolds number 1000). The reactor was tilted during the growth cycle to ensure this high flow velocity. Our experience indicates that biofilms grown at higher flow velocities are more rigid and less susceptible to sloughing. The biofilm did not have the fluffy characteristics of biofilms grown at lower flow velocities, but instead, it consisted of clusters of different sizes separated by voids and channels. Before the measurements were taken, the reactor was leveled and the flow velocity adjusted. Three average flow velocities were used: 0.62, 1.53, and 2.60 cm $sec^{-1}$, corresponding to Reynolds numbers of 100, 300, and 600, respectively. To provide a baseline for mass transport measurements, profiles of local mass transfer coefficient were measured at the same flow velocities in a sterile reactor. As shown in Figure 1, the flow velocity did not have a significant impact on the local mass transfer coefficient in the bulk liquid under those conditions. The variations noted in mass transfer coefficients were between 0.00030 and 0.00034 m $sec^{-1}$. In general, the mass transfer coefficient remained constant until the electrode was 15 μm from the substratum. From this point, we measured a sudden drop in local mass transfer coefficient to less than 50% of its value in the bulk. Although the measurement at the wall could not be performed because of technical difficulties, the shapes of the profiles in Figure 1 suggest that the mass transfer coefficient approaches zero at the wall, which corresponds well with the results reported by Yang and Lewandowski (1995). This effect was expected based upon the fact that the flow velocity near the surface decreases to zero, with the consequence that the convective mass transport rate transport of ferricyanide is restricted by the wall.

Profiles of dissolved oxygen and local mass transfer co-

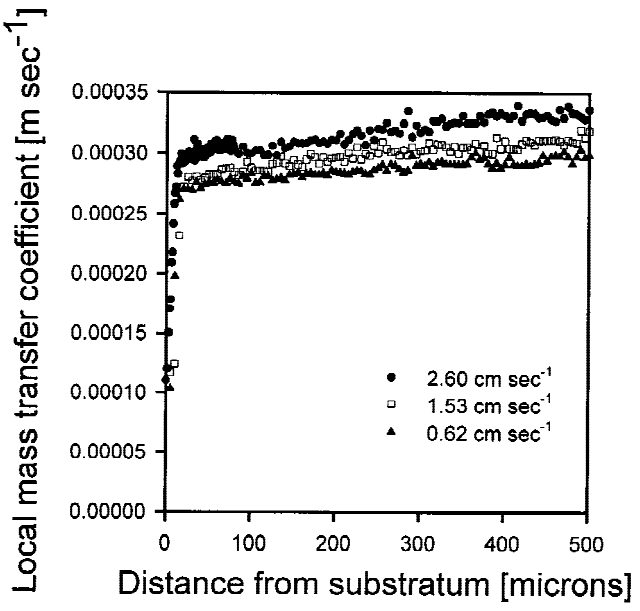


**Figure 1.** Local mass transfer coefficient profiles collected in a sterile reactor at three average flow velocities; 0.62, 1.53, and 2.60 cm $sec^{-1}$. The magnitude of the local mass transfer coefficient remained constant until 15 μm from the substratum. At this point, the wall effect caused a sudden drop in the local mass transfer coefficient.

efficients measured in the presence of the biofilm are shown in Figures 2, 3, and 4. The profiles in Figure 2 were collected at a selected location through a thin cluster, approximately 70 microns thick. When flow velocity was increased from 0.62 cm $sec^{-1}$ to 1.53 cm $sec^{-1}$, the *DBL* thickness decreased from 370 to 60 μm. The oxygen concentration in the bulk solution was close to 6 mg $L^{-1}$ and was depleted inside the biofilm at the lower flow velocity. It is customary to normalize the limiting current when comparing mass transfer rates (Gao et al., 1995; Macpherson et al., 1994).

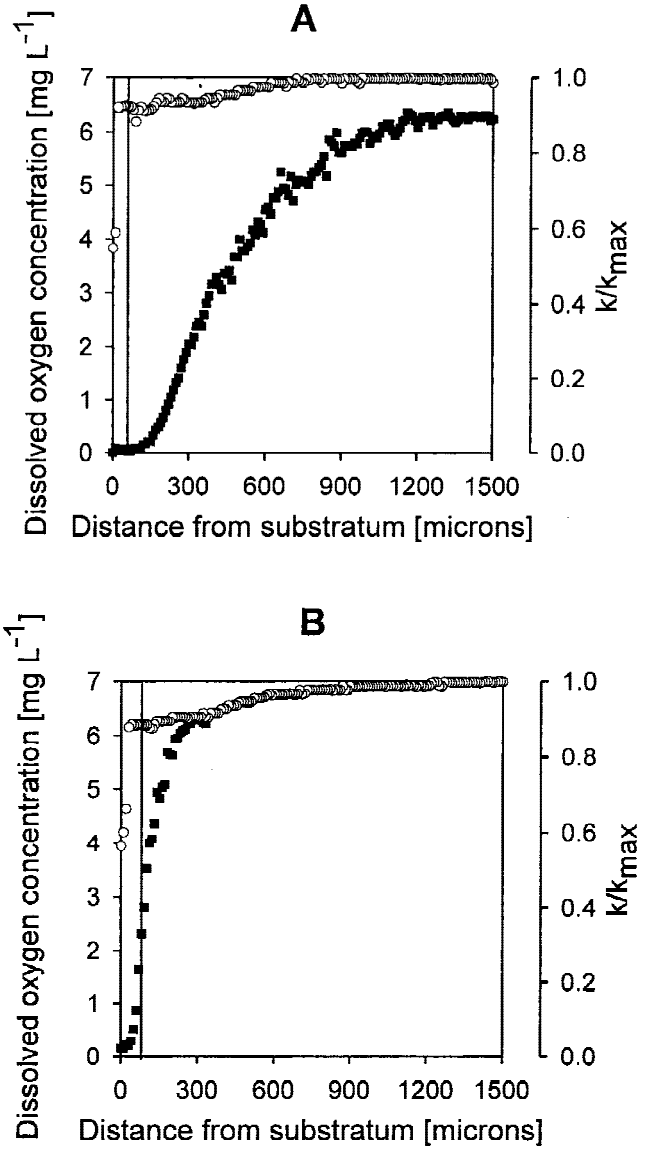


**Figure 2.** Profiles of oxygen and local mass transfer coefficient through a thin biofilm cluster. (■ Dissolved oxygen, ○ Local mass transfer coefficient). The vertical line marks the observed thickness of the biofilm. Profiles of dissolved oxygen and local mass transfer coefficient were collected at flow velocities of **(A)** 0.62 cm $sec^{-1}$ and **(B)** 1.53 cm $sec^{-1}$. At distances less than 30 μm, the wall effect caused the local mass transport coefficient to decrease. The biofilm thickness was 70 μm in this location. $k/k_{max}$ was only slightly affected by the presence of the biofilm until a distance less than 30 μm from the substratum. This is simlar to what is presented in Figure 1 for a sterile reactor.

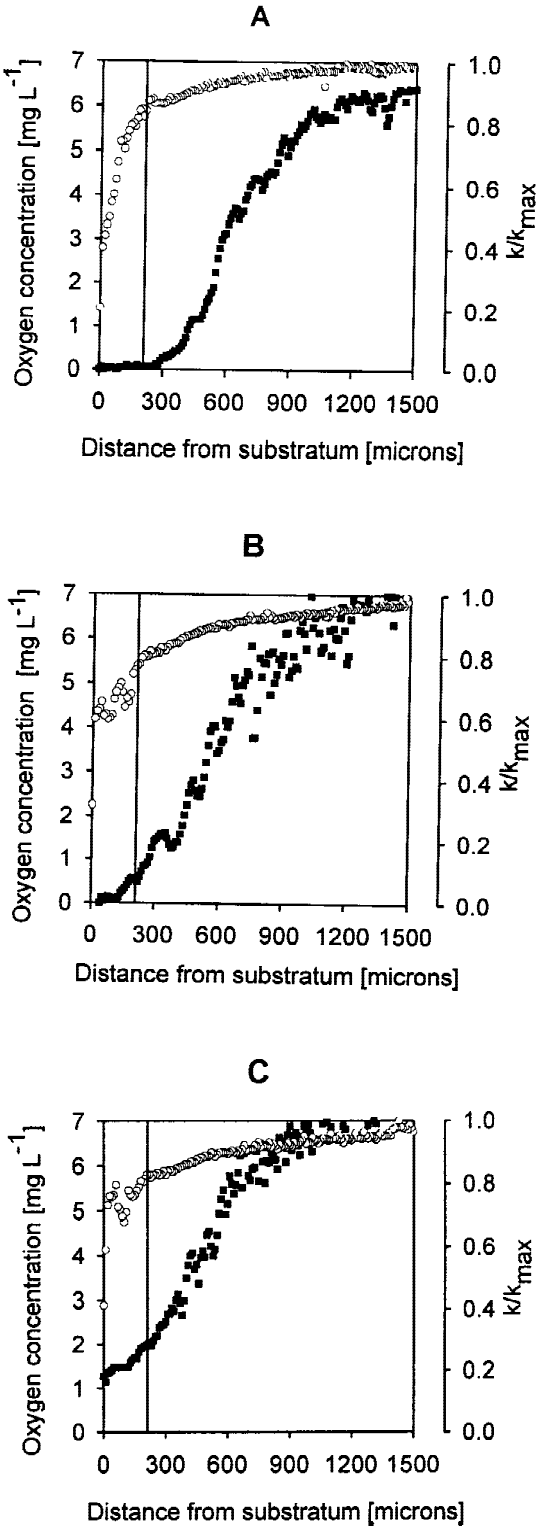


**Figure 3.** Profiles of oxygen and local mass transfer coefficient through an interstitial void (■ Dissolved oxygen, ○ Local mass transfer coefficient). The solid vertical line represents the approximate position of the biofilm surface. Profiles of dissolved oxygen and local mass transfer coefficient were collected at flow velocities of **(A)** 0.62 cm $sec^{-1}$, **(B)** 1.53 cm $sec^{-1}$, and **(C)** 2.60 cm $sec^{-1}$. The measurements were done in an interstitial void, 200 μm thick. The flow velocity had a significant influence on both profiles. A 10–20% reduction of the local mass transfer coefficient was observed through the mass boundary layer. $k/k_{max}$ reached a value of 0.8–0.9 at the level of the biofilm surface, and decreased to less than 0.4 near the substratum.

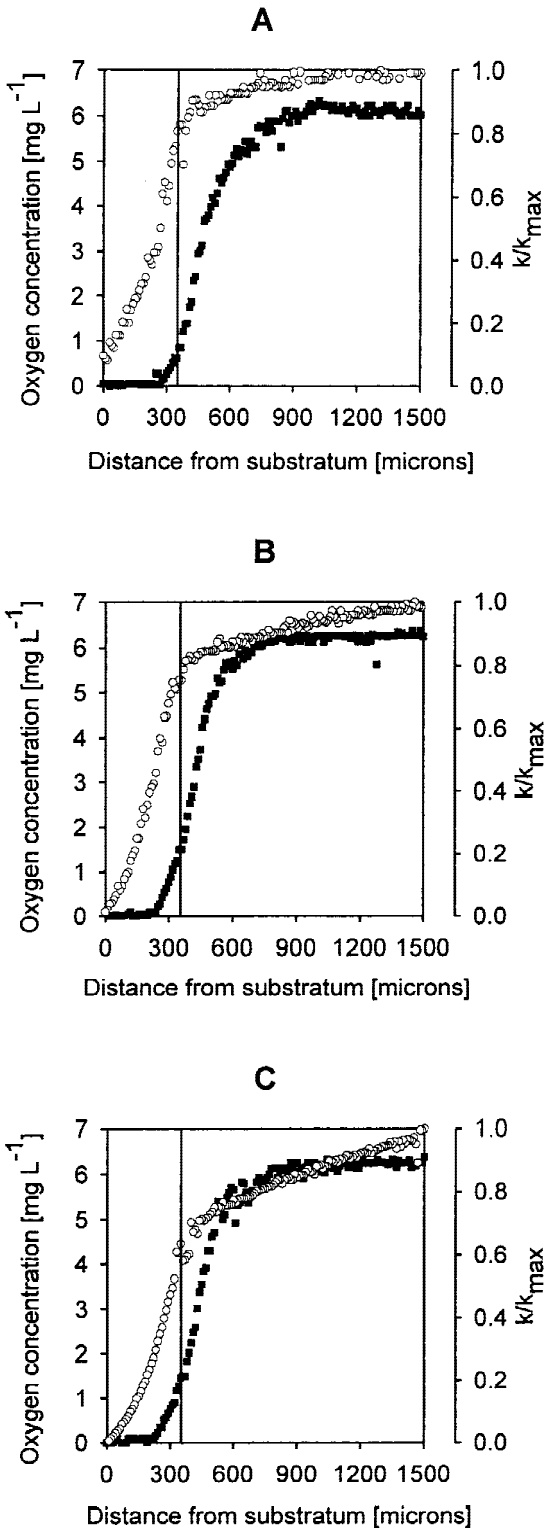


**Figure 4.** Profiles of oxygen and local mass transfer coefficient through a 350 μm thick biofilm cluster (■ Dissolved oxygen, ○ Local mass transfer coefficient). The solid vertical line represents the approximate position of the biofilm surface. Profiles of dissolved oxygen and local mass transfer coefficient through microbial clusters were collected at flow velocities of **(A)** 0.62 cm sec$^{-1}$, **(B)** 1.53 cm sec$^{-1}$, and **(C)** 2.60 cm sec$^{-1}$. The flow velocity had minimal influence on the shape of both profiles. The local mass transfer coefficient at the biofilm surface was 80% of its bulk value. It decreased gradually through the biofilm and reached zero near the substratum.

We normalized the limiting current by dividing each readout by the highest current measured for each profile (reflecting the local mass transfer coefficient in bulk liquid). The results indicate that the local mass transfer coefficient near the biofilm surface was approximately 90% of its value in the bulk. A rapid decrease in the local mass transfer coefficient ($k/k_{max} = 0.5$) was monitored at a distance less than 30 μm from the substratum, which was probably caused by the presence of the wall (see Fig. 1). These results indicate that convection was active both inside and outside the biofilm.

The profiles presented in Figure 3 were measured in a void between two clusters approximately 200 μm thick. The bulk flow velocity was expected to significantly influence the oxygen concentration at this location. At a flow velocity of 0.62 cm sec$^{-1}$, the entire interstitial void was depleted of oxygen, as shown in Figure 3A. By increasing the flow velocity to 2.60 cm sec$^{-1}$ (Fig. 3C), the void became fully penetrated, with an oxygen concentration at the bottom greater than 1 mg L$^{-1}$. The oxygen concentration in the bulk liquid was approximately 6 mg L$^{-1}$. For the flow velocities of 0.62, 1.53, and 2.60 cm sec$^{-1}$, the *DBL* thicknesses were 440, 420, and 260 μm, respectively. The local mass transfer coefficient decreased by 10–20% within the liquid layer, and continues to decrease further below the biofilm surface. In particular, it decreased rapidly for the lowest flow velocity where $k/k_{max}$ reached a value less than 0.4 near the substratum. Comparing the graphs of Figures 3B and C with Figure 3A shows that the extent of local mass transfer coefficient reduction through the interstitial void depends on the flow velocity. The local mass transfer coefficient measured for the flow velocity of 2.60 cm sec$^{-1}$ was consistently higher and less uniform than for both 0.62 cm sec$^{-1}$ and 1.53 cm sec$^{-1}$.

The results of the oxygen and local mass transfer coefficient profiles measured across a 350 μm thick cluster are shown in Figure 4. Increasing the velocity from 0.62 to 2.60 cm sec$^{-1}$ did not significantly change the oxygen concentration gradient inside the biofilm, thus indicating a dense and active biofilm. There was a 200 μm thick anaerobic layer in the lower region of the cluster. For the flow velocities of 0.62 and 1.53 cm sec$^{-1}$, the local mass transfer coefficient at the biofilm surface was $k/k_{max} = 0.8$, and decreased gradually to values near zero at the substratum. The *DBL* thicknesses were 200 and 140 μm for these two velocities, respectively. For the flow velocity of 2.60 cm sec$^{-1}$, $k/k_{max}$ was between 0.6 and 0.7 at the biofilm surface and was significantly lower than for the lower flow velocities. $k/k_{max}$ again decreased gradually through the biofilm and reached zero at the substratum. In this case, the *DBL* thickness was 140 μm.

Figures 2, 3, and 4 show that the slope of the local mass transfer coefficient increases with increasing flow velocity. This effect is more prounounced above the cell clusters than in the void. This effect was not observed in the clean reactor (Fig. 1), and the reasons for this are unknown. The results in Figures 2, 3, and 4 indicate a complex pattern of mass

transport inside the biofilm. If cells and extracellular polymers were uniformly distributed throughout a cell cluster, and no convection occurred, we would expect a constant local mass transfer coefficient within these aggregates. However, Figure 4 shows that the local mass transfer coefficient decreases gradually inside a cluster, approaching zero near the substratum. The local mass transfer coefficient is a function of the effective diffusivity of ferricyanide and of the thickness of the boundary layer surrounding the tip of the microelectrode. A change in either of these two parameters will cause a change in the local mass transfer coefficient. The gradual decrease in the local mass transfer coefficient through the biofilm cluster can be caused by a gradual increase in the biofilm density. As the density increases, mass transfer resistance increases while the effective diffusivity, as well as the local mass transfer coefficient, decrease. It has been reported in the literature that the density of some biofilms increases towards the substratum. Zhang and Bishop (1994b) determined that the densities in the bottom layers of a heterotrophic biofilm were 5–10 times higher than those in the top layers. Fu et al. (1994) determined the effective diffusivity of oxygen in different layers of a biofilm, showing that it was 25–90% lower than the diffusivity of oxygen in water.

Experiments are currently in progress in our lab to verify the hypothesis that the effective diffusivity decreases towards the bottom of the biofilm. A local mass transfer coefficient profile has been measured through a biofilm under stagnant conditions. The local mass transfer coefficient decreased gradually within clusters, approaching zero near the bottom, similar to the profiles collected in a flow field (Fig. 4). Under stagnant conditions, the thickness of the boundary layer surrounding the microelectrode tip is constant, and the only parameter that can cause the reduced local mass transfer coefficient is the effective diffusivity.

Tortuosity and porosity also influence the effective diffusivity. Zhang and Bishop (1994a) reported that for a biofilm with porosities of 0.84–0.93 in the top layers and 0.58–0.67 in the bottom layer, the tortuosity factor increased from 1.2 in the top layer to 1.6 in the bottom layer. In the same biofilm, the ratio of the effective diffusivity to the diffusivity in the bulk solution decreased from 68–81% in the top layer and 38–45% in the bottom layer. Zhang and Bishop (1994a) defined pores as space between clusters. In their model, the clusters obstructed the transport of substrate thereby causing tortuosity. The concept of porosity and tortuosity can be applied on a smaller scale to clusters where cells obstruct the transport of substrate. Substrate transport to cells in the bottom layer of a biofilm is more likely to occur around rather than through the cells. Hence, the cells cause tortuosity. Regions with higher concentrations of cells will have higher tortuosity and lower porosity than regions containing less cells. Zhang and Bishop (1994a) calculated effective diffusivity as $D_e = (\epsilon/\kappa)\, D_w$ where $D_e$ is the effective diffusivity, $\epsilon$ is the porosity ($\epsilon < 1$), $\kappa$ is the tortuosity factor ($\kappa > 1$), and $D_w$ is the diffusivity in water. From this equation, it is evident that if the porosity decreases and/or the tortuosity increases towards the bottom of the biofilm, the effective diffusivity, as well as the local mass transfer coefficient, will decrease.

Yang and Lewandowski (1995) observed irregular profiles of the local mass transfer coefficient inside biofilm clusters. High peaks were believed to be caused by channels inside the clusters which facilitated convective flow. They also observed an increased local mass transfer coefficient just above the biofilm matrix, which was suggested to occur as a result of active movement of the biofilm surface. These two effects were not observed in the experiment detailed in this article. However, the biofilm for the present experiment was grown at a much higher flow velocity, $v = 17$ cm $sec^{-1}$, than that of Yang and Lewandowski (1995), $v = 1.3$ cm $sec^{-1}$. It is well known that biofilms growing at a high flow velocity are relatively rigid and dense (Christensen and Characklis, 1990; Van Loosdrecht et al., 1995). Therefore, it is possible that the secondary heterogeneity monitored by Yang and Lewandowski (1995) was, in the present case, either less evident or absent.

Models of biofilms (Atkinson and Davies, 1974; Rittmann and McCarty, 1978; Wanner and Gujer, 1986) assume the existence of a thin diffusive boundary layer above the biofilm in which the mass transport is dominated by molecular diffusion. If this is true, a sudden drop should be observed in the local mass transfer coefficient when entering this layer. Results presented in this article indicate that convective mass transport is active in the entire system down to the biofilm surface, through the interstitial voids, thin clusters, and in the upper parts of thick clusters. Clusters of 70 $\mu$m and less and interstitial voids between clusters did not significantly influence the local mass transfer coefficient. The only significant reduction in local mass transfer coefficient was observed in thick cell clusters.

It is clear now that the mass transport dynamics in biofilms are much more complex than previously assumed. The following results summarize our findings: (1) Biofilms are heterogeneous and consist of discrete cell clusters separated by interstitial voids; (2) the hydrodynamics in biofilms are controlled by two flow fields, external and internal; and (3) the mass transfer coefficient in biofilms does not behave as predicted by current biofilm models. Although the newly proposed concept of biofilm structure helps to interpret the experimental observations, the new data reveal further dimensions of complexity. We are becoming aware that it may not be possible to completely describe mass transport in biofilms mathematically. Some simplifying assumptions are, therefore, urgently needed to establish empirical equations serving purely practical purposes. It is important that these assumptions are established as a result of experimentation, rather than for computational convenience. Our observations may contribute to this process.

## CONCLUSIONS

The measurements presented in this article were conducted at flow velocities between 0.5 and 2.6 cm $sec^{-1}$. For these

flow velocities, and for the specific experimental conditions employed in our work, we concluded that:

1. Convective mass transport was active near the biofilm/bulk liquid interfaces and in the upper layers of the biofilms.
2. Thin biofilms, 70 μm or less, did not cause any significant changes in local mass transfer resistance.
3. The void spaces between clusters did not cause any significant changes in mass transfer resistance for flow velocities of 1.53 cm $sec^{-1}$ and higher. For a flow velocity of 0.62 cm $sec^{-1}$, the local mass transfer coefficient within the voids decreased gradually towards the bottom.
4. The local mass transfer coefficients in biofilm clusters 350 μm thick and more decreased gradually, approaching zero near the substratum. The decreased local mass transfer coefficient was likely a result of decreased effective diffusivity within the biofilm. It is possible that this decrease in effective diffusivity was due to an increase in the biofilm density near the bottom.

## References


Atkinson, B., Davies, I. J. 1974. The overall rate of substrate uptake (reaction) by microbial films. Part I-A biological rate equation. Trans. Instn. Chem. Engrs. **52**: 248–259.

Bishop, P. L., Rittmann, B. E. 1995. Modeling heterogeneity in biofilms: Report of the discussion session. Wat. Sci. Tech. **32**: 263–265.

Christensen, B. E., Characklis, W. G. 1990. Physical and chemical properties of biofilms, pp. 93–130. In: W. G. Characklis and K. C. Marshall (eds.), Biofilms. Wiley, NY.

Dawson, D. A., Trass, O. 1972. Mass transfer at rough surfaces. Jour. Heat. Mass. Transfer. **15**: 1317–1336.

De Beer, D., Stoodley, P., Roe, F., Lewandowski, Z. 1994a. Effects of biofilm structures on oxygen distribution and mass transport. Biotechnol. Bioeng. **43**: 1131–1138.

De Beer, D., Stoodley, P., Lewandowski, Z. 1994b. Liquid flow in heterogeneous biofilms. Biotechnol. Bioeng. **44**: 636–641.

Fu, Y. C., Zhang, T. C., Bishop, P. L. 1994. Determination of effective oxygen diffusivity in biofilm grown in a completely mixed biodrum reactor. Wat. Sci. Tech. **29**: 455–462.

Gao, X., Lee, J., White, H. S. 1995. Natural convection at microelectrodes. Anal. Chem. **67**: 1541–1545.

Hanratty, T. J. 1991. Use of the polarographic method to measure wall shear stress. Jour. Appl. Electrochem. **21**: 1038–1046.

Hermanowicz, S. W., Schindler, U., Wilderer, P. 1995. Fractal structure of biofilms: New tools for investigation of morphology. Wat. Sci. Tech. **32**: 99–105.

Horn, H., Hempel, D. C. 1995. Mass transfer coefficients for an autotrophic and a heterotrophic biofilm system. Wat. Sci. Tech. **32**: 199–204.

Juhasz, N. M., Deen, W. M. 1993. Electrochemical measurements of mass transfer at surfaces with discrete reactive areas. AIChE Jour. **39**: 1708–1715.

Keevil, C. W., Walker, J. T. 1992. Nomarski DIC microscopy and image analysis of biofilms. Binary **4**: 93–95.

Korber, D. R., James, G. A., Costerton, J. W. 1994. Evaluation of fleroxacin activity against established *Pseudomonas fluorescens* biofilms. Appl. Environ. Microbiol. **60**: 1663–1669.

Larsen, T. A., Harremoës, P. 1994. Combined reactor and microelectrode measurements in laboratory grown biofilms. Wat. Res. **28**: 1435–1441.

Lawrence, J. R., Korber, D. R., Hoyle, B. D., Costerton, J. W., Caldwell, D. E. 1991. Optical sectioning of microbial biofilms. Jour. Bacteriol. **173**: 6558–6567.

Lewandowski, Z., Altobelli, S. A., Fukushima, E. 1993. NMR and microelectrode studies of hydrodynamics and kinetics in biofilms. Biotechnol. Prog. **9**: 40–45.

Lewandowski, Z. 1994. Dissolved oxygen gradients near microbially colonized surfaces, pp. 175–188. In: G. G. Geesey, Z. Lewandowski, and H. C. Flemming (eds.), Biofouling and biocorrosion in industrial water systems. Lewis Publishers, FL.

Lewandowski, Z., Stoodley, P., Altobelli, S. 1995. Experimental and conceptual studies on mass transport in biofilms. Wat. Sci. Tech. **31**: 153–162.

Macpherson, J. V., Marcar, S., Unwi, P. R. 1994. Microjet electrode: A hydrodynamic ultramicroelectrode with high mass transfer rates. Anal. Chem. **66**: 2175–2179.

Revsbech, N. P. 1989a. Microsensors: Spatial gradients in biofilms. In: W. G. Characklis and P. A. Wilderer (eds.), Structure and function of biofilms. Wiley, NY.

Revsbech, N. P. 1989b. An oxygen microsensor with a guard cathode. Limnol. Oceanogr. **34**: 474–478.

Revsbech, N. P., Jørgensen, B. B. 1986. Microelectrodes: Their use in microbial ecology, pp. 293–352. In: K. C. Marshall (ed.), Advances in microbial ecology. Plenum, NY.

Rittmann, B. E., McCarty, P. L. 1978. Variable-order model of bacterial-film kinetics. J. Env. Eng. Div. **104**: 889–900.

Siegrist, H., Gujer, W. 1985. Mass transfer mechanisms in a heterotrophic biofilm. Wat. Res. **19**: 1369–1378.

Stoodley, P., DeBeer, D., Lewandowski, Z. 1994. Liquid flow in biofilm systems. Appl. Environ. Microbiol. **60**: 2711–2716.

Van Loosdrecht, M. C. M., Eikelboom, D., Gjaltema, A., Mulder, A., Tijhuis, L., Heijnen, J. J. 1995. Biofilm structures. Wat. Sci. Tech. **32**: 35–43.

Wanner, O., Gujer, W. 1986. A multispecies biofilm model. Biotechnol. Bioeng. **28**: 314–328.

Welty, J. R., Wicks, C. E., Wilson, R. E. 1976. Fundamentals of momentum, heat, and mass transfer, 2nd edition. Wiley, NY.

Wolfaardt, G. M., Lawrence, J. R., Robarts, R. D., Caldwell, S. J., Caldwell, D. E. 1994. Multicellular organization in a degradative biofilm community. Appl. Environ. Microbiol. **60**: 434–446.

Yang, S., Lewandowski, Z. 1995. Measurement of local mass transfer coefficient in biofilms. Biotechnol. Bioeng. **48**: 737–744.

Zhang, T. C., Bishop, P. L. 1994a. Evaluation of tortuosity factors and effective diffusivities in biofilms. Wat. Res. **28**: 2279–2287.

Zhang, T. C., Bishop, P. L. 1994b. Density, porosity, and pore structure of biofilms. Wat. Res. **28**: 2267–2277.